



# Riverine Discharge and Phytoplankton Biomass Control Dissolved and Particulate Organic Matter Dynamics over Spatial and Temporal Scales in the Neuse River Estuary, North Carolina

Alexandria G. Hounshell<sup>1,2</sup> · Stephen R. Fegley<sup>1</sup> · Nathan S. Hall<sup>1</sup> · Christopher L. Osburn<sup>3</sup> · Hans W. Paerl<sup>2</sup>

Received: 19 October 2020 / Revised: 10 May 2021 / Accepted: 13 May 2021  
© Coastal and Estuarine Research Federation 2021

## Abstract

Estuaries function as important transporters, transformers, and producers of organic matter (OM). Along the freshwater to saltwater gradient, the composition of OM is influenced by physical and biogeochemical processes that change spatially and temporally, making it difficult to constrain OM in these ecosystems. In addition, many of the environmental parameters (temperature, precipitation, riverine discharge) controlling OM are expected to change due to climate change. To better understand the environmental drivers of OM quantity (concentration) and quality (absorbance, fluorescence), we assessed both dissolved OM (DOM) and particulate OM (POM) spatially, along the freshwater to saltwater gradient and temporally, for a full year. We found seasonal differences in salinity throughout the estuary due to elevated riverine discharge during the late fall to early spring, with corresponding changes to OM quantity and quality. Using redundancy analysis, we found DOM covaried with salinity (adjusted  $r^2 = 0.35$ , 0.41 for surface and bottom), indicating terrestrial sources of DOM in riverine discharge were the dominant DOM sources throughout the estuary, while POM covaried with environmental indicators of terrestrial sources (turbidity, adjusted  $r^2 = 0.16$ , 0.23 for surface and bottom) as well as phytoplankton biomass (chlorophyll-*a*, adjusted  $r^2 = 0.25$ , 0.14 for surface and bottom). Responses in OM quantity and quality observed during the period of elevated discharge were similar to studies assessing OM quality following extreme storm events suggesting that regional changes in precipitation, as predicted by climate change, will be as important in changing the estuarine OM pool as episodic storm events in the future.

**Keywords** Particulate organic matter · Dissolved organic matter · Riverine discharge · Global change · Multivariate statistics · Estuaries

## Introduction

Estuaries encompass the transition from freshwater to saltwater and are important and dynamic sites for the production, transformation, and storage of nutrients and organic matter

(OM), prior to export to the coastal ocean (Paerl et al. 1998; Raymond and Bauer 2001; Vlahos and Whitney 2017). Due to their transitional nature, estuaries contain complex mixtures of terrestrially derived and autochthonously produced OM, each of which have unique molecular structures, characteristics, and bioavailabilities (Asmala et al. 2018; Markager et al. 2011; Osburn et al. 2012). OM dynamics in estuaries, including the sources and composition of OM (allochthonous vs. autochthonous), physical and biological degradation and production in situ, mixing with the oceanic waters, and transport of OM through estuarine ecosystems are expected to change under future climate conditions, primarily due to changes in precipitation and resulting riverine inflow (Canuel et al. 2012; Singh et al. 2019). Long-term studies in estuaries that measure OM quantity and quality, however, are few but are needed to fully understand how OM dynamics in these ecosystems may respond to future environmental change (Canuel et al. 2012).

OM is often divided into two pools operationally defined by filtration; here, the dissolved OM (DOM) pool is any

---

Communicated by Paul A. Montagna

---

Alexandria G. Hounshell  
alexgh@vt.edu

<sup>1</sup> Institute of Marine Sciences, University of North Carolina-Chapel Hill, 3431 Arendell St, Morehead City, NC 28557, USA

<sup>2</sup> Present address: Department of Biological Sciences, Virginia Tech, 926 W. Campus Dr, Blacksburg, VA 24061, USA

<sup>3</sup> Department of Marine, Earth, and Atmospheric Sciences, North Carolina State University, 2800 Faucette Dr, Raleigh, NC 27695, USA

organic substance passing through a 0.7  $\mu\text{m}$  nominal pore-size glass fiber filter while the particulate OM (POM) pool is any organic component retained on that filter. Generally, DOM is considered to be more bioavailable to heterotrophic microorganisms than POM and frequently occurs at much greater concentrations (McCallister et al. 2006; Raymond and Bauer 2001). Both DOM and POM can be derived from either allochthonous (terrestrial, wetland) or autochthonous (planktonic, benthic) sources. The composition, relative dominance, and sources of these two pools change down-estuary in response to physical, chemical, and biological processes along the estuarine salinity gradient (Huguet et al. 2009; McCallister et al. 2006). These biogeochemical responses are largely dependent on individual estuarine characteristics including size, geomorphology, stratification patterns, and watershed area, making it difficult to generalize OM patterns and processes across multiple estuarine ecosystems (Canuel et al. 2012).

For coastal plain estuaries specifically, the OM pool in the landward, freshwater reach of the estuary is largely composed of terrestrial, humic-like material flushed from the surrounding watershed and primarily delivered to the estuary by riverine discharge (Fellman et al. 2010; Middelburg and Herman, 2007; Savoye et al. 2012). Seaward, as salinity and mixing with marine waters increase, the estuarine OM pool becomes characteristically more autochthonous and planktonic-like. This shift in OM composition down-estuary can be due to several processes including: removal of terrestrial-like OM via photochemical and biological degradation; flocculation or sedimentation; dilution with marine waters; and production of autochthonous-like OM by phytoplankton and microbial assemblages (Asmala et al. 2016; Brym et al. 2014; Fellman et al. 2010; Osburn et al. 2012). While both OM pools undergo dilution, transformation, and production processes along the estuarine salinity gradient, the DOM pool often retains more of its allochthonous, terrestrial character than the POM pool (McCallister et al. 2006; Osburn et al. 2012).

Despite previous studies that assessed the DOM and/or POM pool in estuaries (i.e., Brym et al. 2014; Dixon et al. 2014; Loh et al. 2006; McCallister et al. 2006; Osburn et al. 2012; Raymond and Bauer 2001; Thibault et al. 2019), few studies have simultaneously assessed the quantity and quality of both the DOM and POM pools over the predominate temporal (i.e., seasonal) and spatial (i.e., down-estuary) gradients within estuaries. Due to the physical differences and various filtration, isolation, and sample preparation constraints, simultaneously measuring DOM and POM quality can be difficult, time-consuming, and expensive. The use of absorbance and fluorescence in conjunction with concentration measurements over the past several decades has allowed rapid and broad characterization of both the quantity and quality of colored

and fluorescent dissolved OM (CDOM and FDOM, respectively) in a variety of aquatic ecosystems, including estuaries (Coble 1996; Jaffé et al. 2014; Markager et al. 2011; Osburn et al. 2012; Stedmon and Markager 2005). While originally limited to measuring DOM, more recently, base-extraction techniques initially developed for the extraction of fluorescent OM from soils, have been applied to seston collected in aquatic systems (i.e., base-extracted particulate organic matter, BEPOM; Brym et al. 2014; Osburn et al. 2012). These two techniques, fluorescent DOM and fluorescent BEPOM, can now be used simultaneously to assess the relative quality of both the DOM and POM pools in aquatic ecosystems on relevant spatial and temporal scales.

These techniques (concentration, absorbance, fluorescence) have been successfully used in synoptic studies of our study site, the Neuse River Estuary (NRE), North Carolina (NC), USA (Brym et al. 2014; Dixon et al. 2014; Osburn et al. 2012). Over annual timescales, these studies have demonstrated a consistent shift from allochthonous OM in the upper estuary to autochthonous, planktonic-like OM in the mid- to lower-estuary for both DOM (Dixon et al. 2014) and POM (Brym et al. 2014). Following flooding related to passage of Hurricane Irene (August 2011), however, both OM pools shifted to more allochthonous-like material throughout the estuary, suggesting that storm events, characterized by elevated riverine flow, have a dramatic impact on the sources and distribution of OM throughout the estuary (Osburn et al. 2012). What has yet to be demonstrated is how longer-term changes in precipitation (i.e., increased occurrence, intensity and duration of precipitation events) will influence the sources, composition, transformation, and transport of both DOM and POM through the estuarine continuum. This is particularly relevant to the southeastern USA, where observed (Paerl et al. 2020) and predicted increases in precipitation events and duration are occurring due to climate change, particularly in the fall and winter (Easterling et al. 2017).

The goal of this study was to advance our understanding of annual (July 2015–July 2016) dynamics of DOM and POM in the eutrophic, river-dominated NRE, using established optical and chemical measurements. We achieved this goal using multivariate statistical analyses to determine correlative relationships between measurements of OM quantity and quality and environmental parameters to understand potential drivers of DOM and POM along the estuarine continuum. Additionally, results from this study were used to assess how climate change, which may lead to changes in riverine discharge, may influence OM quality and quantity in this coastal plain estuary. Results further our understanding of the environmental co-variables, processes, and function of DOM and POM in estuarine environments and provide insight into how estuarine carbon cycling may change under future climate conditions.

## Materials and Methods

### Study Site and Sampling Methods

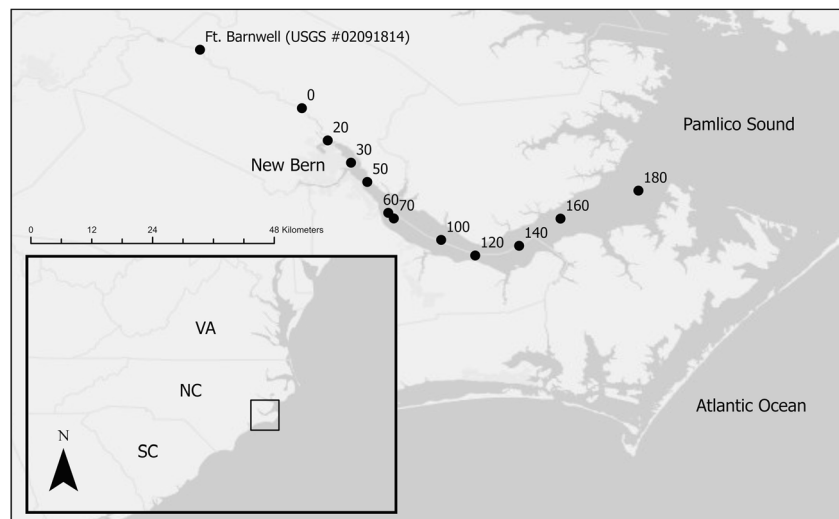
The NRE is a eutrophic, river-dominated, micro-tidal estuary located in the coastal plain of eastern North Carolina (NC), USA (Fig. 1). The Neuse River flows through the urbanized Raleigh-Durham area and several downstream municipalities (Goldsboro, Kinston, and New Bern, NC) before entering the estuary. Watershed land use is characterized by agriculture (concentrated animal feeding and row crop operations), wetlands, and forests (Bhattacharya and Osburn 2020; Rothenberger et al. 2009). Due to the diverse land use, a variety of nutrient and OM sources are present within both the Neuse River and NRE watersheds (Bhattacharya and Osburn 2020; Osburn et al. 2016). The estuary drains into Pamlico Sound, a large ( $5335 \text{ km}^2$ ) lagoonal system with weak tidal exchange with the Atlantic Ocean. In the NRE, negligible tides (amplitude  $\sim 0.04 \text{ m}$ ) lead to residence times of  $\sim 5\text{--}8$  weeks which are largely controlled by freshwater discharge (Peierls et al. 2012). Long residence time provides ample time for phytoplankton and associated microbial assemblages to utilize both inorganic and organic nutrients discharged to the NRE (Christian et al. 1991; Luettich et al. 2000).

Samples for physical, chemical, biological, and OM analyses were collected as part of the Neuse River Monitoring and Modeling Program (ModMon; <http://paerllab.web.unc.edu/projects/modmon/>) conducted by the University of North Carolina – Chapel Hill, Institute of Marine Sciences (UNC-CH IMS) (Paerl et al. 2018). Samples were collected for a full year from 20 July 2015 to 28 July 2016; bi-weekly from March through October and monthly from November through February. For each of the 22 sampling dates, samples were

collected at 11 stations in the NRE spanning the upstream-most location of salinity intrusion (station 0) to the mouth of the estuary (station 180) (Fig. 1). Temperature (Temp), salinity (Sal), turbidity (Turb), and percent saturation of dissolved oxygen (%DO) were measured at surface (0.2 m below surface) and bottom (0.5 m above bottom) depths using a YSI 6600 multi-parameter, water quality sonde (Hall et al. 2013). Surface (0.2 m below surface) and bottom (0.5 m above bottom) water samples were collected for chemical, biological, and OM analyses at each of the 11 stations. Collected samples were maintained in the dark at ambient temperature and returned to UNC-CH IMS within  $\sim 6$  h of collection. Samples were filtered through pre-combusted ( $450^\circ\text{C}$ , 4 h) GF/F glass fiber filters (0.7  $\mu\text{m}$  nominal pore size). The filtrate was collected and stored frozen at  $-20^\circ\text{C}$  in the dark until dissolved nutrient and DOM quantitative and qualitative analysis (Appendix S1). Filters were collected and stored frozen at  $-20^\circ\text{C}$  in the dark until chlorophyll-*a* (Chl *a*) analysis, conducted within 1 month of collection, and POM quantitative and qualitative analyses, as described below.

Neuse River discharge data were obtained 26 km upstream from the head of the NRE (station 0) at USGS gaging station #02091814 located at Ft. Barnwell, NC (Fig. 1). Discharge data were scaled up by 31% to account for drainage from the area of un-gaged watershed (Peierls et al. 2012). Median discharge, along with the 25th and 75th percentiles, were calculated by USGS for data collected from 1996 to 2019. For data analysis and visualization, samples were divided into five seasonal periods: *Summer 2015* = July 2015–August 2015; *Fall* = September 2015–November 2015; *Winter* = December 2015–February 2016; *Spring* = March 2016–May 2016; and *Summer 2016* = June 2016–July 2016. Samples were also divided into surface (0.2 m below surface) and bottom (0.5 m above bottom) datasets.

**Fig. 1** Map of the Neuse River Estuary (NRE) located in Eastern North Carolina, USA. ModMon sampling locations are designated as stations 0–180. The location of the USGS gage (#02091814) used for riverine discharge data is designated as Ft. Barnwell



## Organic Matter Analysis

DOC concentration ([DOC]) was measured via high-temperature catalytic oxidation on a Shimadzu TOC-5000 analyzer (Peierls et al. 2003). [DOC] quality control checks were conducted using DOC standards (12.5 mg C L<sup>-1</sup>; NSI Lab Solutions, Raleigh, NC) with an analytical uncertainty of 4.4% (Paerl et al. 2018). Total dissolved nitrogen (TDN, analytical uncertainty = 3.6%), nitrate + nitrite (NO<sub>3</sub><sup>-</sup> + NO<sub>2</sub><sup>-</sup>, analytical uncertainty = 4.7%), and ammonium (NH<sub>4</sub><sup>+</sup>, analytical uncertainty = 1.5%) were determined colorimetrically using a Lachat QuickChem flow-injection autoanalyzer (Paerl et al. 2018; Peierls et al. 2003, 2012). Dissolved organic nitrogen ([DON]) was determined by subtracting the dissolved inorganic nitrogen species (DIN, as NO<sub>3</sub><sup>-</sup> + NO<sub>2</sub><sup>-</sup> + NH<sub>3</sub><sup>+</sup>) from TDN (analytical uncertainty = 3.6%; Paerl et al. 2018). Particulate organic carbon ([POC]) and particulate nitrogen ([PN]) were determined on one set of collected filters via high temperature combustion on a Costech ECS 4010 elemental analyzer, after vapor acidification (HCl) to remove inorganic carbon (Paerl et al. 2018). Atropine standards were used to develop a calibration curve (70.56% C and 4.64% N) for analysis. [POC] and [PN] analytical uncertainty was 6.2% and 7.5% (Paerl et al. 2018).

Samples for absorbance and fluorescent BEPOM were extracted following Osburn et al. (2012). Briefly, seston on collected filters was extracted using 10 mL of 0.1 M NaOH and stored in the dark at 4 °C for 24 h. Samples were then neutralized with concentrated HCl (~ 100 µL) to measured neutral pH (~ 7.0) and filtered through 0.2 µm porosity, polyethersulfone (PES) filters. Filtered extracts were immediately analyzed for absorbance and fluorescence as described below. For absorbance and fluorescence, DOM and neutralized BEPOM samples were filtered through 0.2 µm pore size, PES filters immediately prior to analysis to ensure optical consistency (Appendix S1).

Absorbance spectra for filtered DOM and extracted POM samples were measured on a Shimadzu UV-1700 Pharma-Spec spectrophotometer. Absorbance spectra were corrected using a Nanopure water blank measured at the beginning of each day of analysis. All samples with > 0.4 raw absorbance units at 240 nm were diluted, and final results were corrected for dilution (Osburn et al. 2012). Absorbance values at 254 nm (A<sub>254</sub>) were converted to Napierian absorbance coefficients (a<sub>254</sub>, m<sup>-1</sup>) (Spencer et al. 2013). Specific UV absorbance (SUVA<sub>254</sub>) (L mg<sup>-1</sup> C m<sup>-1</sup>) was calculated as decadal A<sub>254</sub>/[OC] (as [DOC] or [POC], respectively) for each sample (Weishaar et al. 2003).

Fluorescence spectra (i.e., excitation-emission matrices, EEMs) were measured on a Varian Cary Eclipse spectrofluorometer. Excitation wavelengths were scanned from 240 to 450 nm at 5 nm increments, and emission wavelengths were scanned from 300 to 600 nm at 2 nm increments. All sample

EEMs were blank corrected using fluorescence spectra obtained for Nanopure water on the same day of sample analysis, which also removed most Rayleigh and Raman scatter. Additional scattering was removed using in-house scripts written in Matlab. Instrument excitation and emission corrections were applied to each sample in addition to corrections for inner-filtering effects, calibrated against the Raman signal of Nanopure water, and standardized to quinine sulfate equivalents (Q.S.E.) (Murphy et al. 2013).

The humification index (HIX) and biological index (BIX) were calculated from measured fluorescence spectra and used as indicators of the relative quality of OM in estuaries from more terrestrial, humic-like OM to more biological, autochthonously produced OM (Huguet et al. 2009). HIX is the ratio of the H (435–480 nm) and L (300–345 nm) regions of fluorescence measured at an excitation wavelength of 254 nm. HIX is indicative of the degree of humification and aromaticity of the fluorescent OM in a sample (Table 1). BIX is calculated as the ratio between the β (380 nm) (Peak M) and α (430 nm) (Peak C) regions of fluorescence measured at an excitation wavelength of 310 nm. BIX is an indicator of autochthonous, recently produced fluorescent OM (Huguet et al. 2009) (Table 1). Molar ratios of DOC:DON and POC:PN were additionally calculated as indicators of OM quality.

## Chlorophyll- $\alpha$ Analysis

Phytoplankton biomass was measured as Chl  $\alpha$  using a modified version of EPA fluorometric method 445.0 (Arar and Collins 1997). Briefly, collected filters were extracted overnight in 90% acetone followed by processing in a tissue grinder. Extracts were analyzed un-acidified on a Turner Designs TD-700 fluorometer with a narrow bandpass filter.

## Statistical Analyses

Previous studies have demonstrated the unique geochemical properties of DOM and POM in estuarine ecosystems and have used multivariate statistical analyses to identify environmental controls on DOM and POM composition before and after a hurricane event (Osburn et al. 2012). Following this study, we divided the collected data into separate DOM and POM datasets for statistical analysis in addition to the collected environmental data used to explain variation in the DOM and POM datasets, respectively. Thus, we characterized environmental data as temperature, salinity, turbidity, %DO, and Chl  $\alpha$ ; the DOM dataset as all concentration ([DOC], [DON], DOC:DON), absorbance (a<sub>254</sub>, SUVA<sub>254</sub>), and fluorescence (HIX, BIX) measurements for the DOM pool; and the POM dataset as all concentration ([POC], [PN], POC:PN), absorbance (a<sub>254</sub>, SUVA<sub>254</sub>), and fluorescence (HIX, BIX) measurements for the POM pool. For the redundancy analysis, the environmental dataset was used as the explanatory

**Table 1** Previously characterized fluorescent indices (humification index (HIX) and biological index (BIX)) as identified in the literature Huguet et al. (2009)

Fluorescent identification	Excitation, emission wavelength (nm)	Characterization
Humification index (HIX)	254, 435–480/300–345	> 16: Humic, terrestrial-like 6–10: Mainly humic, terrestrial-like with some weak autochthonous influence 4–6: Little humic, terrestrial-like influence with greater autochthonous influence < 4: Autochthonous, biological sources
Biological index (BIX)	310, 380/430	> 1: Autochthonous, biological sources 0.8–1: Relatively large, autochthonous contribution 0.7–0.8: Small autochthonous contribution 0.6–0.7: Very low autochthonous contribution

variables with the DOM and POM datasets used as the response variables, respectively. In addition, we separated each dataset (environmental, DOM, POM) into surface and bottom samples to explore the influence of stratification on DOM and POM in this eutrophic estuary. Prior to conducting multivariate statistical analyses, each dataset (environmental surface and bottom; DOM surface and bottom; POM surface and bottom) was examined individually for collinearity among variables. Collinear variables ( $r^2 > 0.80$ ) were removed from subsequent multivariate analyses (Table 2).

Principal components analysis (PCA) was conducted on each individual dataset (environmental surface, environmental bottom, DOM surface, DOM bottom, POM surface, and POM bottom) to assess relationships and correlations among the various measurements collected. PCA was conducted on each dataset after normalization (z-scores) and removal of collinear variables ( $r^2 > 0.80$ ). Redundancy analysis (RDA) is a combination of PCA and multiple linear regression and allows for an explanatory (i.e., environmental data) and response (i.e., DOM or POM datasets respectively) dataset to assess underlying patterns in the data. RDA was conducted utilizing forward, stepwise addition, to select environmental

variables (Temp, Sal, Turb, %DO, Chl *a*) that explained the most variation in the response datasets (Borcard et al. 2018). Variables were included based on a pre-defined alpha-level ( $\alpha < 0.05$ ) and stopped when the adjusted  $r^2$  exceeded the global model. Reverse, step-wise subtraction was used to confirm results.

All multivariate statistical analyses were conducted in R version 4.0.2. PCA and RDA were conducted using the vegan package for R (<https://cran.r-project.org/web/packages/vegan/index.html>). All data corrections and calculations for absorbance and fluorescent indices were conducted in Matlab R2017b. Environmental, DOM, and POM data collected as part of this project are available on the Environmental Data Initiative (Hounshell et al. 2021).

## Results

### Environmental and organic matter parameters

From late fall 2015 to early spring 2016, Neuse River discharge was elevated with values about twice the long-term

**Table 2** Parameters that were not collinear ( $r^2 < 0.80$ ) nor highly correlated in principal component analysis (PCA) space and were included in subsequent multivariate analyses for each data set. Abbreviations include: dissolved organic matter, DOM; particulate organic matter, POM; dissolved organic carbon concentration, DOC; particulate organic

carbon concentration, POC; dissolved organic nitrogen concentration, DON; molar ratios of DOC and DON, DOC:DON; molar ratios of POC and particulate nitrogen (PN), POC:PN; SUVA at 254 nm, SUVA<sub>254</sub>; absorbance measured at 254 nm,  $a_{254}$ ; biological index, BIX; and humification index, HIX

Environmental, surface	Environmental, bottom	DOM, surface	DOM, bottom	POM, surface	POM, bottom
Salinity	Salinity	DOC	DOC	POC	POC
Temperature	Temperature	DOC:DON	DON	POC:PN	POC:PN
Turbidity	Turbidity	SUVA <sub>254</sub>	DOC:DON	$a_{254}$	$a_{254}$
Chlorophyll- <i>a</i>	Chlorophyll- <i>a</i>	BIX	BIX	SUVA <sub>254</sub>	SUVA <sub>254</sub>
	% Dissolved oxygen			HIX	HIX
				BIX	BIX

daily median (Fig. 2). The extended period of elevated riverine discharge resulted in depressed estuarine salinity for both surface and bottom samples at all stations throughout the NRE starting in late fall 2015 (Fig. 3a, c). Temporally, the elevated riverine discharge led to depressed salinity values in both surface and bottom samples in the winter and spring 2016 as compared to the summer and fall 2015, which persisted until summer 2016 (Fig. 3b, d). During the late summer and early fall of 2015, Chl *a* peaks in the surface were distributed throughout the estuary (from station 30 to 180; Fig. 3e). During winter to early spring 2016, however, surface Chl *a* was highest in the lower estuary (stations 160–180), with lowest median Chl *a* concentrations throughout the estuary (Fig. 3f, h) followed by a return of surface Chl *a* peaks into the mid-estuary (station 70) during late spring and summer 2016 and an increase in median Chl *a* concentrations throughout the estuary (Fig. 3e, f). Similar patterns were observed in Chl *a* measured in the bottom waters, though bottom water Chl *a* was about half that of the surface waters (Fig. 3g, h).

Spatially, in summer 2015, [DOC] was highest in the upper estuary (< 60 km downstream) for both surface and bottom samples (Figs. 4a, c and S3). Following increased riverine discharge in late fall 2015, there was a noticeable increase in [DOC] throughout the estuary, with maximum [DOC] in the upper estuary for both depths (Fig. 4a, c). This was followed by elevated [DOC] throughout the estuary during the winter at all stations in the NRE (Fig. 4a, c). Temporally, surface [DOC], plotted seasonally during the study period, was inversely related to salinity in the estuary (Figs. 3b and 4b) with the highest surface [DOC] in the winter and lower surface [DOC] during the spring and summer 2016. Similar patterns were observed in bottom [DOC] with highest bottom [DOC]

observed in the winter followed by decreasing concentrations in spring and summer 2016 (Fig. 4d). Compared to [DOC], [POC] was lower for all seasons and depths and exhibited less seasonal variation (Fig. 4). Spatially, [POC] visually followed trends observed in the Chl *a* data for both surface and bottom (Figs. 3e–h and 4e–h).

As an indicator of the quality of the two OM pools, the C:N molar ratio, SUVA<sub>254</sub>, BIX, and HIX were plotted spatially down-estuary (Fig. 5) and temporally by season for both surface and bottom DOM and POM (Fig. 6). Overall, dissolved C:N ratios were higher throughout the estuary as compared to particulate C:N ratios with little observed difference in surface and bottom samples (Figs. 5a, b and 6a, b). While there appears to be little variation in DOC:DON down-estuary (Fig. 5a), POC:PN generally decreased down-estuary from ~ 10 in the upper estuary to ~ 6 in the lower estuary (Fig. 5b). Similarly, dissolved SUVA<sub>254</sub> (~ 3–4 L mg<sup>-1</sup> C m<sup>-1</sup>) was higher than particulate SUVA<sub>254</sub> (~ 1–2 L mg<sup>-1</sup> C m<sup>-1</sup>) indicating there was less aromatic, humic-like OM in the POM versus DOM pool (Weishaar et al. 2003; Figs. 5c, d and 6c, d). For DOM SUVA<sub>254</sub>, there was a slight decrease down-estuary, with greater variability in the lower estuary as compared to the upper estuary as well as generally lower SUVA<sub>254</sub> values in the bottom as compared to the surface waters (Fig. 5c). Temporally, there was an increase in DOM SUVA<sub>254</sub> in the winter following increases in discharge (Fig. 6c). For POM SUVA<sub>254</sub>, there was a noticeable decrease in SUVA<sub>254</sub> down-estuary with decreasing variability (Fig. 5d). Seasonally, there was increasing POM SUVA<sub>254</sub> following the increased riverine discharge in addition to increased variability, especially in the winter and spring (Fig. 6d).

For the fluorescent indicators of OM quality (BIX, HIX), there was generally increasing BIX for both DOM and POM

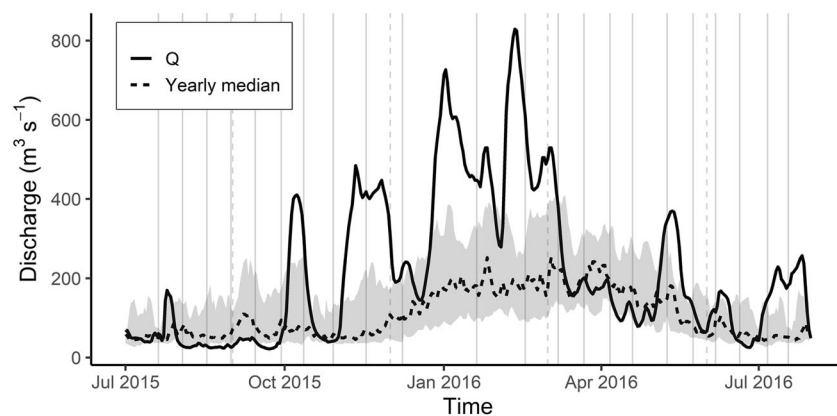


**Fig. 2** Riverine discharge from July 1, 2015–July 31, 2016, measured at the USGS gaging station located 20 km upstream from station 0 at Ft. Barnwell, NC, and scaled to account for the un-gaged fraction of the watershed (31%). Daily discharge measured during the study is plotted in the solid line. The dashed black line represents the median daily discharge calculated from 1996 to 2019. Gray shading extends from the 25th

to 75th percentile of daily discharge calculated from 1996 to 2019. Solid vertical grey lines indicate sampling time points in the NRE during the study period while dashed vertical gray lines indicate seasonal designations (Summer 2015 = July 2015–August 2015; Fall = September 2015–November 2015; Winter = December 2015–February 2016; Spring = March 2016–May 2016; Summer 2016 = June 2016–July 2016)

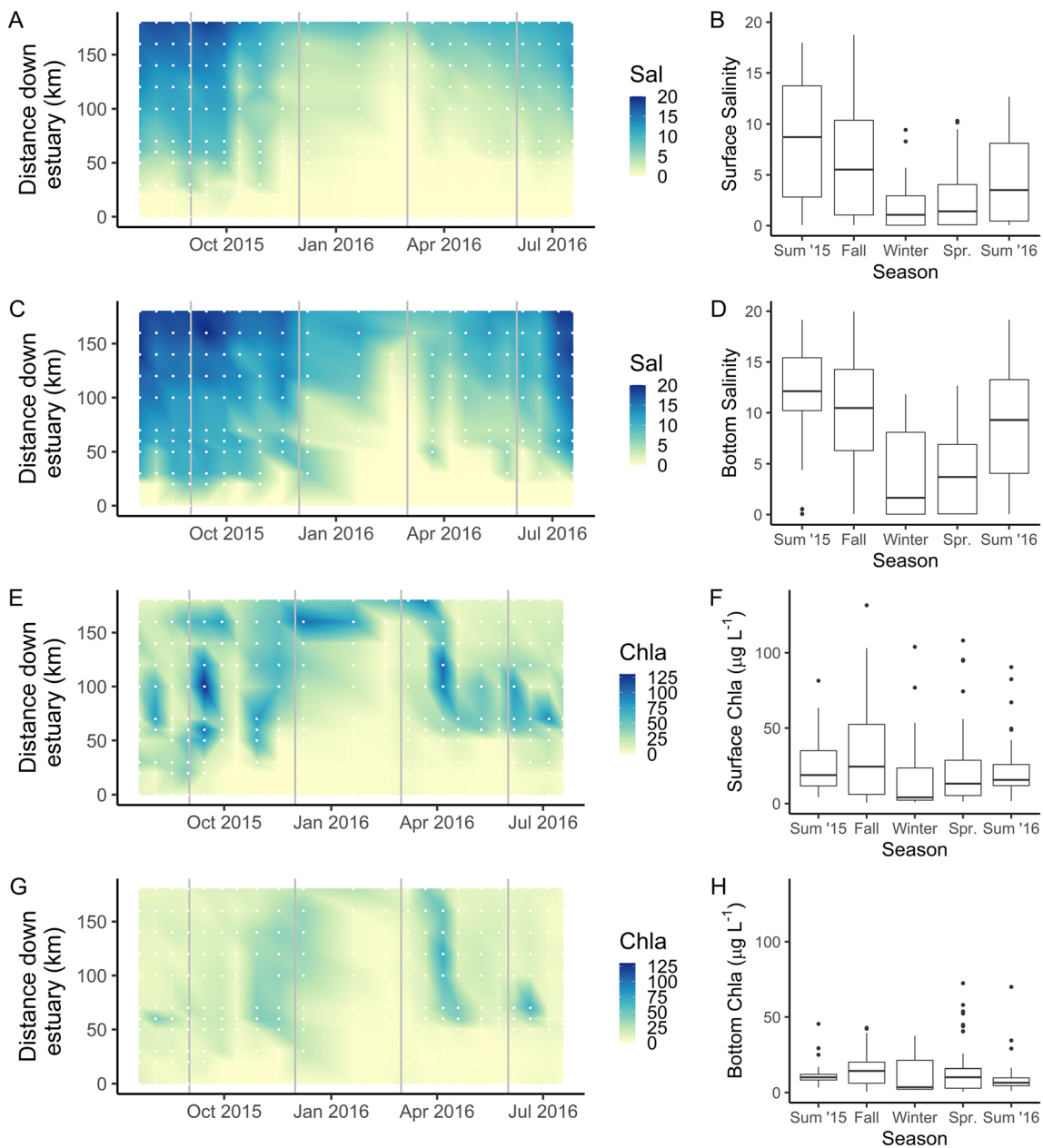


**Fig. 3** Heatmaps for surface and bottom salinity (Sal, **A** and **C**, respectively) and surface and bottom chlorophyll-*a* (Chl *a*,  $\mu\text{g L}^{-1}$ ; **E** and **G**, respectively). Heatmaps were generated from data collected in the NRE from July 2015 to July 2016 at 11 locations throughout the estuary. White dots represent time and location where data was collected. Data were linearly interpolated between sampling points. Gray vertical lines indicate seasonal designations. Seasonal box plots for **B** surface salinity, **D** bottom salinity, **F** surface Chl *a*, and **H** bottom Chl *a*. Seasons were separated as *Summer 2015* (Sum '15; July 2015–

August 2015), *Fall* (September 2015–November 2015), *Winter* (December 2015–February 2016); *Spring* (Spr; March 2016–May 2016), and *Summer 2016* (Sum '16; June 2016–July 2016). Box plots include all surface or bottom samples, respectively, collected during each season for all stations (0–180). For each box plot, the median is represented by the bolded line while the 25th and 75th percentile are represented by the bottom and top of the box, respectively. The whiskers represent the minimum and maximum values ( $1.5 \times$  interquartile range) while outliers are plotted as circles

down-estuary accompanied by decreasing HIX (Fig. 5e–h). For DOM BIX, samples in the upper estuary were largely characterized as very low autochthonous contribution (BIX < 0.6). In the lower estuary, dissolved BIX values increased and were characterized as OM with a small autochthonous contribution (BIX 0.6–0.7; Fig. 5e). Similarly, POM BIX also

increased from low autochthonous contribution in the upper estuary to a small autochthonous contribution in the lower estuary (Fig. 5f). Unlike DOM BIX, POM BIX had much greater variability in the lower estuary, with some samples characterized as autochthonous biological sources (BIX > 1.0). Temporally, DOM BIX was lowest in the winter

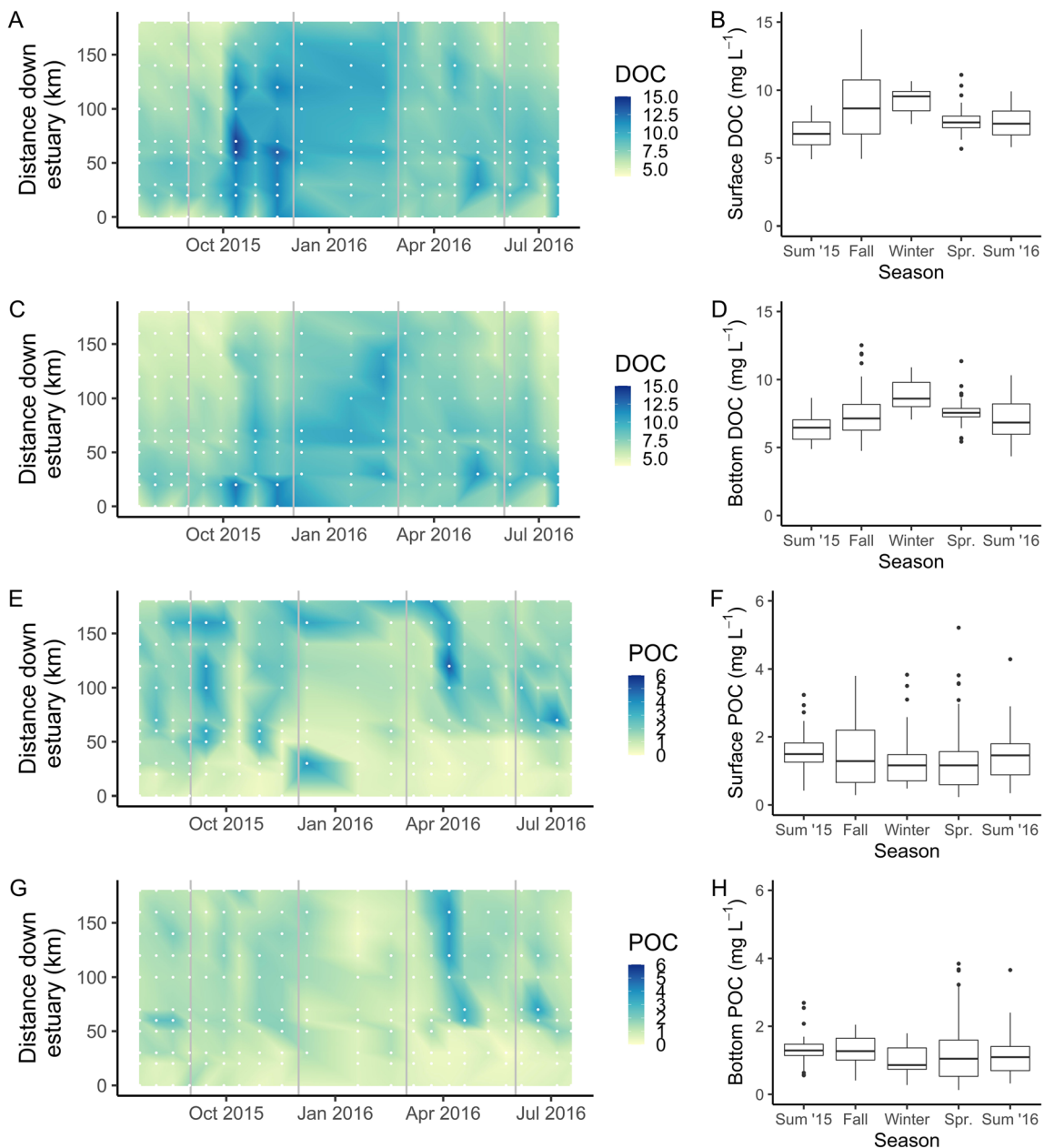


**Fig. 4** Heatmaps for surface and bottom dissolved organic carbon (DOC) concentration ( $\text{mg L}^{-1}$ ; **A** and **C**, respectively) and surface and bottom particulate organic carbon (POC) concentration ( $\text{mg L}^{-1}$ ; **E** and **G**, respectively). Heatmaps were generated from data collected in the NRE from July 2015 to July 2016 at 11 locations throughout the estuary. Data were linearly interpolated between sampling points. Gray vertical lines indicate seasonal designations. Seasonal box plots for **B** surface DOC, **D** bottom DOC, **F** surface POC, and **H** bottom POC. Seasons were separated as *Summer 2015* (Sum '15; July 2015–August 2015), *Fall*

(September 2015–November 2015), *Winter* (December 2015–February 2016); *Spring* (Spr; March 2016–May 2016), and *Summer 2016* (Sum '16; June 2016–July 2016). Box plots include all surface or bottom samples, respectively, collected during each season for all stations (0–180). For each box plot, the median is represented by the bolded line while the 25th and 75th percentile are represented by the bottom and top of the box, respectively. The whiskers represent the minimum and maximum values ( $1.5 \times$  interquartile range) while outliers are plotted as circles

following increased riverine discharge while POM BIX exhibited little seasonal variation but much greater sample variability (Fig. 6e, f). There appeared to be little variation in surface and bottom samples for either DOM or POM BIX. For DOM HIX, the upper estuarine samples were characterized as mainly humic, terrestrial-like ( $\text{HIX} > 10$ ) decreasing to

humic, terrestrial-like with some weak autochthonous influence (HIX 6–10) in the lower estuary (Fig. 5g). Temporally, DOM HIX showed a large increase in the winter, followed by decreasing values from spring to summer 2016 (Fig. 6g). POM HIX was generally lower than DOM with values characterized as humic, terrestrial-like with some weak

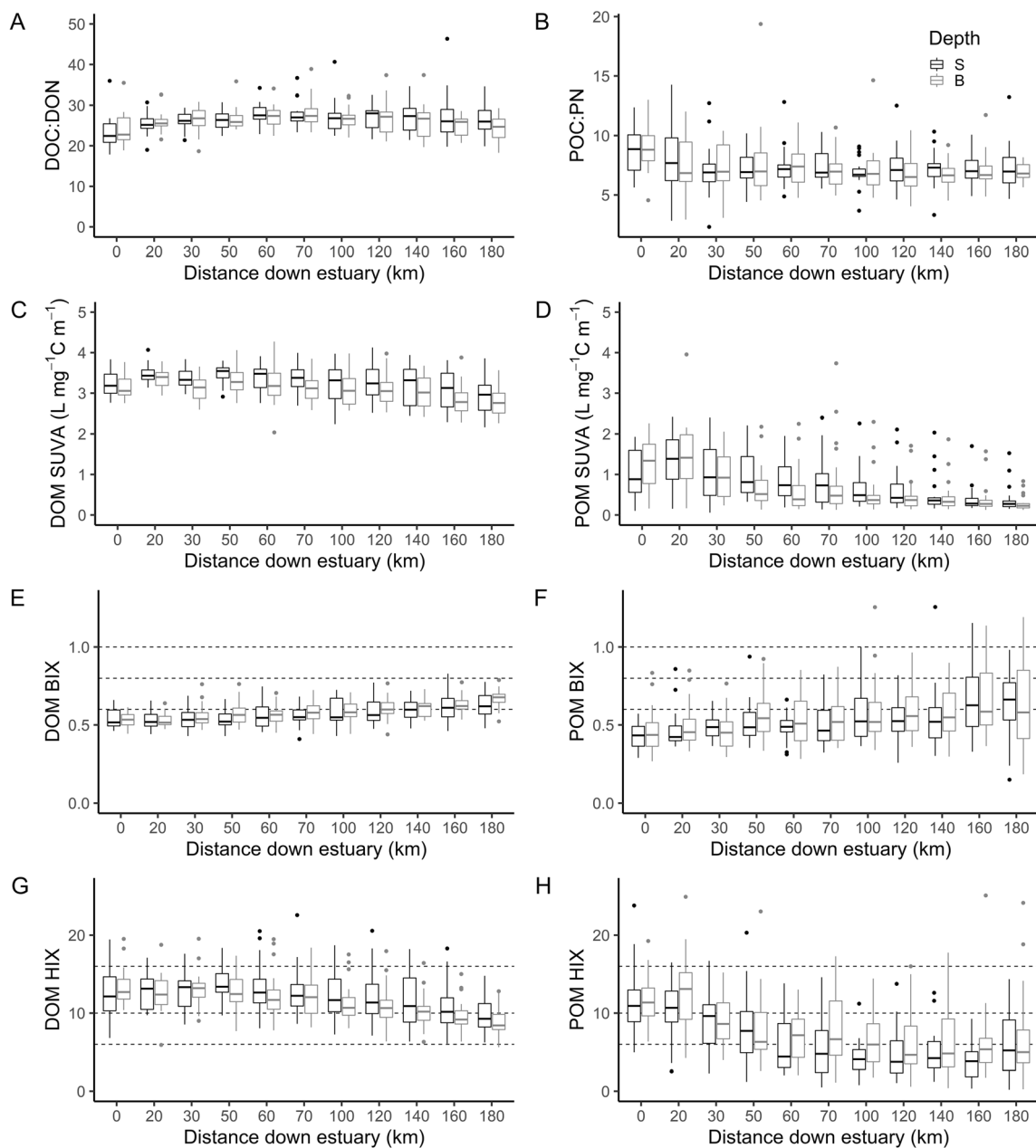


**Fig. 5** Boxplots showing distribution of samples with distance down-estuary for dissolved organic matter (DOM) and particulate organic matter (POM) quality parameters including **A** the molar ratio of dissolved organic carbon (DOC) to dissolved organic nitrogen (DON), DOC:DON; **B** molar ratios of particulate organic carbon (POC) to particulate nitrogen (PN), POC:PN; **C** DOM SUVA<sub>254</sub> ( $L \text{ mg}^{-1} \text{ C m}^{-1}$ ) measured at absorbance 254 nm; **D** POM SUVA<sub>254</sub> ( $L \text{ mg}^{-1} \text{ C m}^{-1}$ ) measured at absorbance 254 nm; **E** DOM biological index (BIX); **F** POM BIX; **G** DOM humification index (HIX); and **H** POM HIX. Note the difference in scale

autochthonous influence in the upper estuary decreasing to little humic, terrestrial-like influence with greater autochthonous influence in the lower estuary (Fig. 5h). Seasonally, there was increasing POM HIX from summer to winter 2015 followed by decreasing values from winter to spring 2016 (Fig. 6h).

for DOC:DON and POC:PN. Each box represents all samples collected at that station throughout the study period (July 2015–July 2016) separated by depth (surface and bottom). For each box plot, the median is represented by the bolded line while the 25th and 75th percentile are represented by the bottom and top of the box, respectively. The whiskers represent the minimum and maximum values ( $1.5 \times$  interquartile range) while outliers are plotted as circles. The horizontal dashed lines correspond to the distinctions for HIX and BIX described in Table 1

Prior to multivariate analysis (PCA, RDA), we tested each dataset (environmental surface, environmental bottom, DOM surface, DOM bottom, POM surface, POM bottom) for collinearity ( $r^2 > 0.80$ ). Several variables within each of the data matrices were collinear ( $r^2 > 0.80$ ) and were removed prior to multivariate statistical analyses. For environmental surface

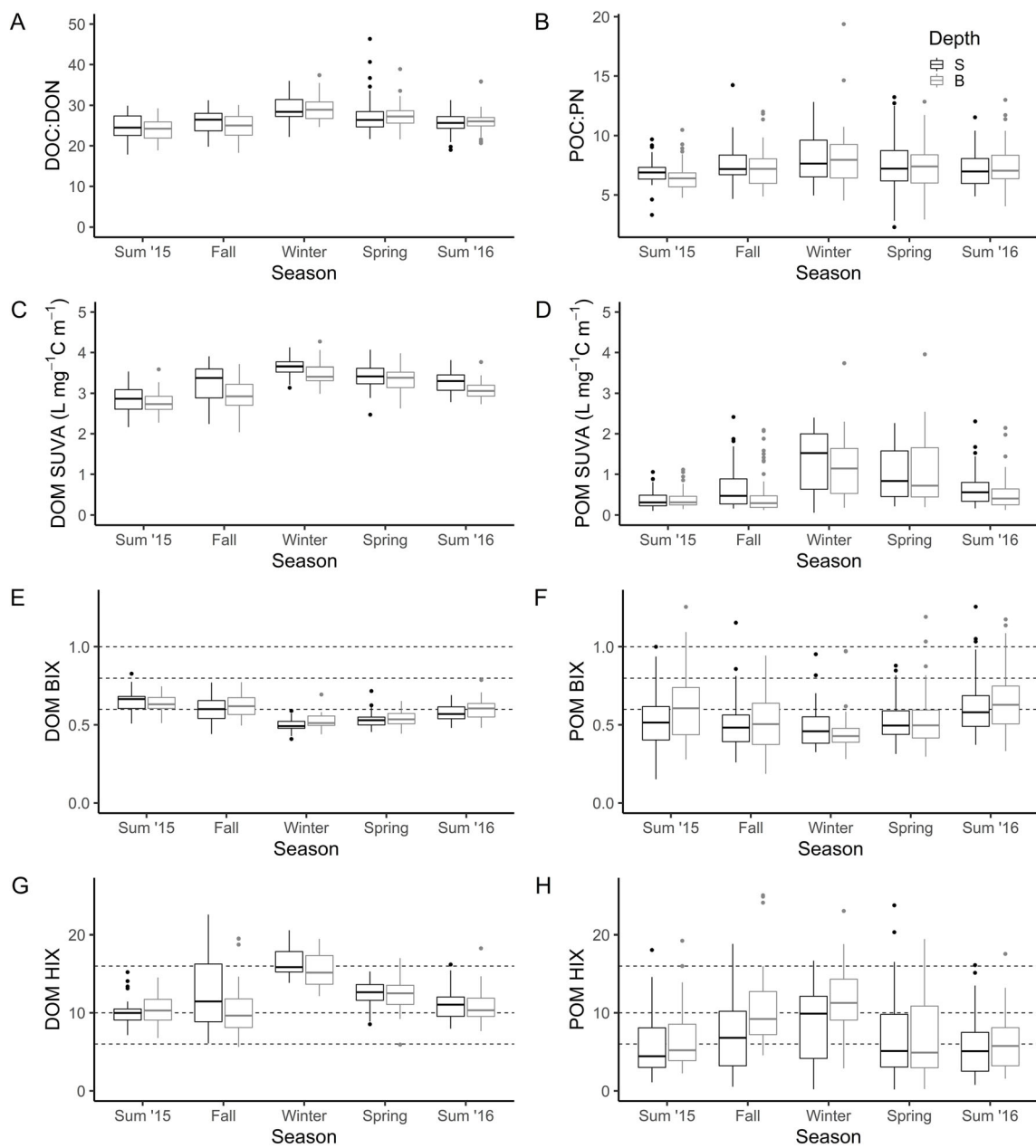


**Fig. 6** Seasonal boxplots for **A** molar ratios of dissolved organic carbon (DOC) to dissolved organic nitrogen (DON), DOC:DON; **B** molar ratios of particulate organic carbon (POC) to particulate nitrogen (PN), POC:PN; **C** dissolved organic matter (DOM) SUVA<sub>254</sub> ( $\text{L mg}^{-1} \text{C m}^{-1}$ ) measured at absorbance 254 nm; **D** particulate organic matter (POM) SUVA<sub>254</sub> ( $\text{L mg}^{-1} \text{C m}^{-1}$ ) measured at absorbance 254 nm, **E** DOM biological index (BIX), **F** POM BIX, **G** DOM humification index (HIX), and **H** POM HIX. Note the difference in scale for the DOC:DON and POC:PN ratios. Samples are divided into season as *Summer 2015* (Sum '15; July 2015–August 2015), *Fall* (September 2015–November

2015), *Winter* (December 2015–February 2016), *Spring* (March 2016–May 2016), and *Summer 2016* (Sum '16; June 2016–July 2016). Samples are also divided into surface (black) and bottom (gray). Each box represents all samples at all stations collected for that season and depth. For each box plot, the median is represented by the bolded line while the 25th and 75th percentile are represented by the bottom and top of the box, respectively. The whiskers represent the minimum and maximum values ( $1.5 \times$  interquartile range) while outliers are plotted as circles. The horizontal dashed lines correspond to the distinctions for HIX and BIX described in Table 1

samples, %DO and Chl *a* were highly correlated in PCA space and therefore, %DO was removed (Fig. S4). Phytoplankton blooms, as measured by peaks in Chl *a*, are often associated with elevated %DO and are a common driver of observed DO

super-saturation in eutrophic surface waters, including in the NRE (O'Boyle et al. 2013 and references within). All environmental parameters were retained for the bottom samples (Fig. S5).

For the DOM datasets (both surface and bottom), there were several parameters which were collinear with [DOC] and were removed (surface: [DON],  $a_{254}$ , HIX; bottom:  $a_{254}$ , SUVA<sub>254</sub>, HIX) (Figs. S6 and S7). Several indicators of humic-like, terrestrial OM ( $a_{254}$ —surface and bottom; SUVA<sub>254</sub>—bottom; HIX—surface and bottom) were correlated with [DOC], indicating that terrestrial, humic-like DOM makes up a significant portion of the total DOM pool in the NRE. Notably, [DON] was strongly correlated with [DOC] in the surface but not in the bottom waters. There were fewer instances of collinearity among POM parameters. Both [POC] and [PN] were collinear for surface and bottom datasets, and thus, [PN] was removed (Figs. S8 and S9), indicating that most POM contained both [POC] and [PN] at fairly consistent ratios.

## Principal Component Analysis

PCA was conducted on each individual data set (environmental surface and bottom; DOM surface and bottom; POM surface and bottom) after normalization (z-scores) and removal of collinear variables (Fig. 7). For each individual data set, PC1 characterized about 40–60% of the variance while PC2 characterized about 20–30% of the variance. Overall, there were few visible differences among seasons, designated as *summer 2015* (July 2015–August 2015), *fall* (September 2015–November 2015), *winter* (December 2015–February 2016), *spring* (March 2016–May 2016), and *summer 2016* (June 2016–July 2016) for any of the six datasets indicating seasonality, as defined broadly above, did not produce any clear patterns in the datasets.

The orientation of variables within PCA space for surface and bottom datasets were similar among different data pools (i.e., environmental, DOM, POM), indicating that there was likely little difference between surface and bottom samples (Fig. 7). A notable exception is the relationship of %DO in the surface and bottom of the environmental dataset. As explained previously, %DO in surface samples was strongly correlated with Chl *a* in PCA space, resulting in the removal of %DO from this dataset. For the bottom data set, %DO was not tightly coupled with Chl *a* and was thus included in the PCA. PCA results for the bottom environmental samples demonstrate that %DO was not strongly correlated with Chl *a* and was oriented 180° from temperature. Consequently, unlike for surface samples where %DO was associated with DO production by phytoplankton, the dominant correlation with %DO in the bottom waters was likely a negative correlation with temperature, reflective of bottom water hypoxia often exhibited in the NRE in the summer (Buzzelli et al. 2002). For the DOM and POM pools, respectively, similar relationships among variables were identified in both the surface and bottom samples, indicating that despite slight differences in

environmental parameters, there were no discernible differences between the OM pools of surface and bottom waters.

There were clear differences in the orientation of indicators of terrestrial-like and autochthonous, planktonic-like OM for both the DOM and POM pools. For the surface DOM pool, BIX, an indicator of autochthonous-like, microbial OM was oriented 180° from SUVA<sub>254</sub>, an indicator of more terrestrial-like allochthonous OM (Fig. 7). Similarly, in surface and bottom POM, BIX was oriented 180° from HIX as well as SUVA<sub>254</sub>. In addition, the orientation of [DOC] and [POC] with various indicators of OM quality can reveal potential sources of OM in the NRE. Specifically, in the DOM pool, [DOC] was oriented opposite of BIX but was correlated with indicators of more allochthonous like material (SUVA<sub>254</sub> for surface; DOC:DON for bottom). In surface and bottom POM, [POC] was most closely aligned with BIX an indicator of autochthonous, microbial-like OM (Fig. 7).

## Redundancy Analysis

Redundancy analysis (RDA) is a combination of PCA and multiple linear regression such that an explanatory dataset (i.e., environmental parameters) is used to explain the variation in a response data matrix (i.e., DOM or POM, respectively). As with PCA, RDA was conducted on separate surface and bottom datasets for DOM and POM, respectively to allow for differences in depth to be identified. For the DOM surface and bottom parameters, salinity was identified as the environmental variable which explained the most variation in DOM followed by temperature (Table 3, left column). For the POM surface dataset, Chl *a* and then turbidity explained the most variability in POM quality and quantity (Table 3, right column). For the POM bottom dataset, turbidity and then Chl *a* explained the most variability. As in the PCA, RDA revealed only slight differences between the DOM and POM pools for surface and bottom samples (Fig. 8). For POM surface samples, a larger percent of the variability in the dataset was explained by Chl *a*, likely due to the larger Chl *a* values measured in the surface versus bottom waters for the NRE (Fig. 3e–h). This result may indicate that phytoplankton contributed a greater percentage to the total POM pool in the surface versus bottom waters, due to periodic bloom formation.

## Discussion

While previous studies have measured either the DOM or POM pools individually or both pools over short temporal (i.e., weeks) or spatial scales (i.e., Brym et al., 2014; Dixon et al. 2014; Loh et al. 2006; McCallister et al. 2006; Osburn et al. 2012; Raymond and Bauer 2001; Thibault et al. 2019),

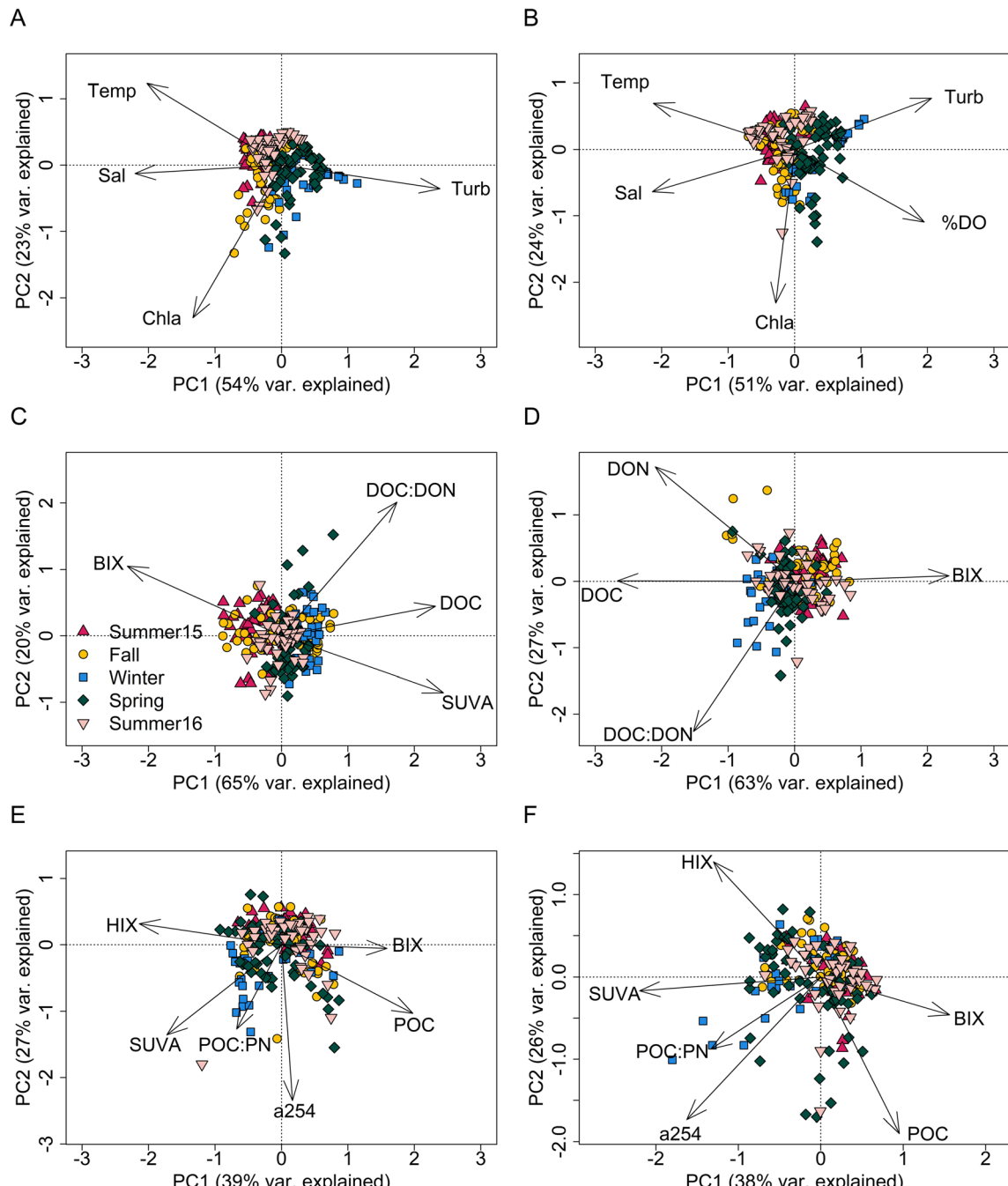


**Fig. 7** Principal component analysis (PCA) results for the **A** environmental surface samples, **B** environmental bottom samples, **C** dissolved organic matter (DOM) surface samples, **D** DOM bottom samples, **E** particulate

organic matter (POM) surface samples, and **F** POM bottom samples. Data points are plotted by season (key in **C**). Arrows represent variable loads

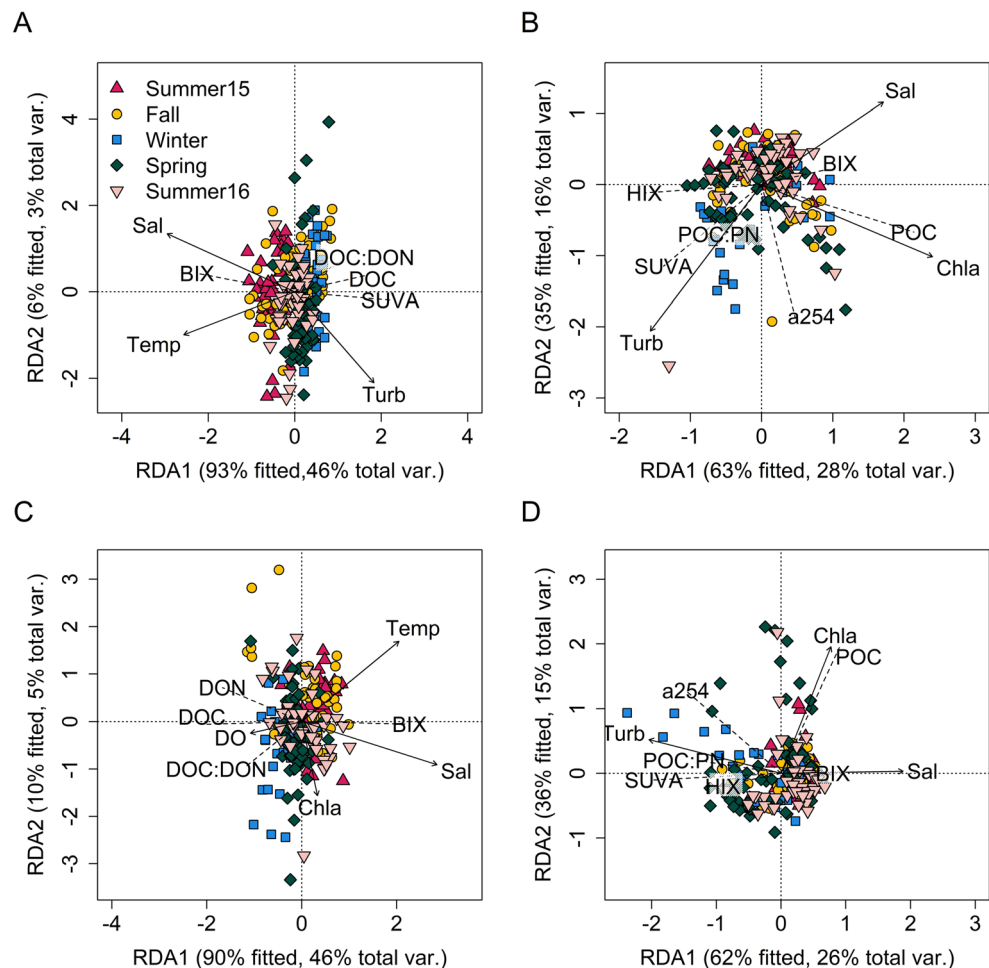
this is one of the first studies to use optical indices (as absorbance and fluorescence) measured for both the DOM and POM pools to assess spatial (i.e., throughout the estuary) and temporal (i.e., seasonal) OM variability. Results from this study, when compared to previous studies of OM variability following storm events (Paerl et al. 2020; Osburn et al. 2012)

as well as under more normal riverine discharge conditions (Brym et al. 2014; Dixon et al. 2014; Peierls et al. 2012), can be used to understand how long-term changes in precipitation patterns, as predicted in the future due to climate change Lehmann et al. (2015) will impact OM cycling in the NRE and similar eutrophic, temperate estuaries.

**Table 3** Redundancy analysis (RDA) results for dissolved organic matter (DOM; surface and bottom) and particulate organic matter (POM; surface and bottom) data. Variables were selected for inclusion based on forward selection and confirmed with reverse selection

DOM surface samples			POM surface samples		
Environmental variable	Cumulative adjusted $r^2$	<i>p</i> value	Environmental variable	Cumulative adjusted $r^2$	<i>p</i> value
Salinity	0.35	0.001	Chlorophyll- <i>a</i>	0.25	0.001
Temperature	0.46	0.001	Turbidity	0.41	0.001
Turbidity	0.49	0.001	Salinity	0.44	0.001
DOM bottom samples			POM bottom samples		
Environmental variable	Cumulative adjusted $r^2$	<i>p</i> value	Environmental variable	Cumulative Adjusted $r^2$	<i>p</i> value
Salinity	0.41	0.001	Turbidity	0.23	0.001
Temperature	0.47	0.001	Chlorophyll- <i>a</i>	0.37	0.001
% Dissolved oxygen	0.49	0.001	Salinity	0.40	0.001
Chlorophyll- <i>a</i>	0.50	0.005			

**Fig. 8** Redundancy analysis (RDA) correlation plots for **A** dissolved organic matter (DOM) surface samples, **B** DOM bottom samples, **C** particulate organic matter (POM) surface samples, and **D** POM bottom samples. Data points are plotted by season (key in C). Organic matter variables (loadings) are displayed as dashed lines. Environmental variables (loadings) are plotted as solid arrows



## Spatial and Temporal Variability in the OM Pool Is Driven by Salinity and Chlorophyll *a*

Spatially, we observed decreasing [DOC] down-estuary but increasing [POC] over an annual time scale (July 2015–July 2016; Figs. 4a, c and S3), indicating differing sources, sinks, and processes for these two pools in the NRE. By assessing OM quality, we were able to identify the potential sources of DOM and POM throughout the estuary, as terrestrial, humic-like allochthonous material versus planktonic-like, autochthonous material. Specifically, using absorbance and fluorescence-based metrics, we found decreases in allochthonous, humic-like OM down-estuary for both DOM and POM (SUVA<sub>254</sub>, HIX) along with increases in autochthonous, planktonic-like material (BIX; Fig. 5). These observed spatial gradients in OM quality were stronger for POM as compared to DOM, as observed in previous studies (Paerl et al. 2020), and consistent with the much greater overall variability in the POM versus the DOM pool throughout the estuary (Fig. 5). This implies that generally the DOM is more stable than POM, for the most part being conservatively mixed across the salinity gradient, while POM is attuned to biological production in the estuary. Our results for the NRE support the concept of the estuary as a filter where OM is comprised of changing combinations of allochthonous and autochthonous material where humic-like, allochthonous material dominates the upper-estuary and transitions proportionally to more planktonic-like, autochthonous material in the lower estuary (Canuel and Hardison 2016; Dürr et al. 2011).

PCA results showed a similar story with [DOC] clustered with indicators of humic-like, terrestrial OM (i.e., DOC:DON, SUVA<sub>254</sub>) in PCA space as compared to [POC] which was clustered with indicators of planktonic-like, autochthonous OM (BIX) (Fig. 7). While the spatial analysis described above suggests changes in the DOM and POM pools through the estuary, PCA results highlight the dominant sources and processes in these two pools: with DOM predominately characterized as humic-like, allochthonous material and POM predominately characterized as planktonic-like, autochthonous OM. Other studies have highlighted similar associations with the DOM and POM pools in estuarine ecosystems following storm events (Letourneau and Medeiros, 2019; Lu and Liu, 2019).

Quantitatively, RDA demonstrated that salinity explained the greatest variability in both the surface and bottom DOM datasets ( $r^2 = 0.35$  and 0.41, respectively). Salinity is a tracer of freshwater flow in estuaries, where lower salinity corresponds to more river-dominated, terrestrial processes and higher salinity is indicative of more marine, autochthonous processes. In RDA space, the orientation of [DOC] was about 180° opposite of salinity and was clustered with indicators of terrestrial, humic-like OM (i.e., SUVA<sub>254</sub>, DOC:DON); conversely, indicators of autochthonous like DOM (i.e., BIX) are

oriented with high salinity (Fig. 8). These results illustrate that riverine processes dominate DOM throughout the estuary, with some contribution of autochthonous-like DOM in the lower estuary.

Conversely, RDA identified Chl *a* and turbidity as explaining the most variation in the POM dataset (Table 2). This suggests that both autochthonous (Chl *a* production) and allochthonous (high turbidity riverine water) were important sources of POM. For both the surface and bottom POM datasets, [POC] was closely related to Chl *a* in RDA space (Fig. 8). Both [POC] and Chl *a* were oriented in the same direction as indicators of autochthonous-like POM (BIX) and oriented opposite of more terrestrial, humic-like POM (a<sub>254</sub>, SUVA<sub>254</sub>, HIX, POC:PN). Turbidity was also identified as an important indicator of POM variability in both the surface and bottom datasets and was most closely associated with indicators of terrestrial, humic-like POM (i.e., POC: PN, SUVA<sub>254</sub>, a<sub>254</sub>). This indicates that while [POC] is most closely aligned with autochthonous POM produced by phytoplankton, [POC] characterized as humic-like, allochthonous material is likely derived from riverine water characterized by high turbidity (Figs. 8, S10, and S11). Indeed, turbidity and the associated indicators of allochthonous POM are oriented 180° from salinity. Turbidity, especially in the fresher waters of the upper- and mid-estuary, has been shown to play an important role in the POM cycle in estuarine ecosystems as fresh and saltwater meet and result in a turbidity maximum which is characterized by high rates of flocculation and POM formation before being sedimented out (Canuel and Hardison 2016; Dürr et al. 2011). It is likely that the NRE follows similar patterns where POM is largely comprised of terrestrial-like material in the upper and mid-estuary with a transition to predominantly autochthonous-like POM in the mid- to lower-estuary following flocculation in the turbidity maximum and phytoplankton production in the mid- to lower-estuary (Fig. 3). The location of this POM processing likely changes temporally based on the extent of freshwater influence within the estuary.

Temporally, we found some evidence to indicate OM processes differed with season, although this was largely obscured by increased riverine discharge in the late fall 2015 to early spring 2016 (Fig. 2). There was a clear increase in terrestrial, humic-like DOM and POM during the winter when riverine discharge was an important influence in both the upper and lower estuary (Fig. 4), yet there was no obvious seasonal variation in PCA or RDA results for either the DOM or POM pools or by depth (surface or bottom; Figs. 7 and 8). The increased riverine discharge during winter 2015 was naturally coupled with decreasing seasonal autochthonous primary production typically observed in the NRE (Pinckney et al. 1998), potentially confounding any patterns due to seasonality that would otherwise have been identified during a more normal period of riverine discharge. Despite this, RDA results suggest

temperature, a proxy for seasonal variability, may be an important driver for the DOM pool. Specifically, we found temperature explained a small amount of variation in the DOM pool for both surface and bottom samples (adjusted  $r^2 = 0.09$  and 0.06, respectively). During a year when riverine discharge was closer to the long-term median, we might expect temperature and thus seasonality to play a more important role in the DOM pool. For the POM pool, temperature was not identified as an important environmental variable. Although phytoplankton production exhibits a pronounced seasonality with a summer maximum and winter minimum (Pinckney et al. 1998), a similar pattern of grazing mortality mutes the phytoplankton biomass response and causes weak seasonality of Chl  $a$  in the NRE (Pinckney et al. 1998; Litaker et al. 2002). Thus, the lack of a strong temperature impact on POM is consistent with what we know about seasonality of phytoplankton biomass.

In addition to analyzing spatial variability in OM downstream as well as temporal variability throughout the year, we also examined differences between surface and bottom samples for both OM pools. Estuarine stratification, driven by layering of fresh, riverine water over saltier, marine water, periodically led to notable differences in surface and bottom water quality (i.e., salinity, temperature, turbidity, %DO; Figs. 3, S11, and S12). Therefore, we expected distinct differences in the quantity and quality of the DOM and POM pools with depth. However, PCA and RDA conducted on separate data sets of surface and bottom samples indicated little difference in either DOM or POM quantity and quality with depth (Figs. 5 and 6). Notably, RDA identified Chl  $a$  (adjusted  $r^2 = 0.25$ ) followed by turbidity (adjusted  $r^2 = 0.16$ ) as the two most important variables for explaining POM variability in the surface waters while for the bottom dataset, turbidity (adjusted  $r^2 = 0.23$ ) then Chl  $a$  (adjusted  $r^2 = 0.14$ ) was identified. The differences in the adjusted  $r^2$  values were relatively small and likely reflect the higher Chl  $a$  and lower turbidity in the surface versus bottom waters (Figs. 3 and S10).

Finally, elevated riverine discharge during the fall and winter resulted in depressed salinity values throughout the water column during winter 2015 and spring 2016 (Fig. 3), which mixed the water column in the upper- and mid-estuary, compared to the lower estuary. Indeed, during winter when riverine discharge was elevated we saw reduced stratification intensity (estimated by subtracting bottom density from surface density following Hall et al. 2015) down to station 100 as compared to previous seasons (Summer 2015, Fall 2015; Fig. S12). Similarly, there was reduced stratification intensity at all stations in spring 2016 (Fig. S12). Although vertical salinity stratification occurs in the NRE, the estuary is shallow and susceptible to mixing by wind events (Luetich et al. 2000) which often homogenizes OM properties (Dixon et al. 2014). Consequently, periods of stratification that last more than a couple of weeks are uncommon. Specifically, the

estuary can fully mix, homogenizing surface and bottoms waters, but then re-stratify within a few days or even hours (Hall et al. 2015). Hence, another possible reason for a lack of vertical differences in DOM and POM quality may be that the time scales of the rate processes acting on DOM and POM quantity and quality (multiple weeks to months) are slow compared to stratification-destratification cycles (days to weeks).

## Climatic Changes Leading to Changes in Estuarine DOM and POM

A clear result of this study is the role riverine discharge can play in altering the DOM and POM pools throughout the estuary. Understanding how seasonal and climatic variability (i.e., temperature, storm events, variable riverine discharge) influence DOM and POM loading and cycling in estuarine ecosystems is particularly important as many of these seasonal and climatic variables are expected to change in the future as a result of climate change (Canuel et al. 2012; Easterling et al. 2017; Janssen et al. 2016). As demonstrated by this and other studies conducted in the river-dominated NRE, changes in riverine discharge, as modulated by precipitation, will have a substantial influence on how the estuary receives, processes, and transports terrestrial and autochthonous OM in the future (Hounshell et al. 2019; Osburn et al. 2012, 2019; Paerl et al. 2018; Rudolph et al. 2020).

Specifically, in addition to following storm events, increases in riverine discharge associated with climatic shifts in precipitation patterns could result in drastic changes to the OM pool in this and similar river-dominated estuaries. During the winter of 2015–2016, elevated riverine discharge led to reduced salinities in the NRE, similar to those following passage of Hurricane Matthew in 2016 (Hounshell et al. 2019), leading to changes in the concentration and composition of both OM pools, but particularly the DOM pool. As demonstrated following Hurricane Matthew, the change in composition in the OM pool was likely caused by hydrologic connectivity of the river's main stem to adjacent riparian wetlands in the lower coastal plain (Rudolph et al. 2020). The increase in wetland-derived DOM had a direct impact on the transport of OM into the downstream Pamlico Sound, switching the system from a CO<sub>2</sub> sink to a CO<sub>2</sub> source (Osburn et al. 2019). We hypothesize that a key regulator of OM flushed into the NRE during elevated riverine flow, exemplified in winter 2015–2016, is due to this same hydrologic connectivity, and resulted in similar changes to OM processing downstream of the NRE. This indicates that not only do single extreme storm events have the potential to drastically change OM and carbon cycling in these ecosystems (Rudolph et al. 2020), but longer-term climatic changes such as increasing frequency and duration of precipitation events will as well.

Indeed, we can compare results from this study (Summer 2015–Summer 2016) to previous studies using similar concentration, absorbance, and fluorescence indices to assess DOM under more average riverine discharge conditions (2010–2011; Dixon et al. 2014). The additional freshwater in 2015–2016 led to higher [DOC] and more terrestrial-like OM (i.e., HIX) observed in the estuary, especially in the later fall early winter following elevated riverine discharge in 2015–2016, with little difference in SUVA<sub>254</sub> between studies (Fig. S13). These comparisons confirm that hydrology is the key driver of carbon and DOM transfer in this system, both following storm events but also following longer-term, seasonally driven increases in riverine discharge.

Similarly, for the POM pool we hypothesize the elevated riverine discharge in winter 2015–2016 was high enough to result in enhanced flushing of phytoplankton biomass (i.e., autochthonous POM) out of the NRE and replaced by the influx of terrestrial-like POM from the watershed. Our results show that high discharge events can cause these changes outside of a hurricane event. Indeed, visual analysis of salinity and Chl *a* plotted spatially down-estuary and temporally through time indicates decreased surface salinity throughout the estuary following increased riverine discharge in the late fall 2015 which was associated with low Chl *a* in the upper estuary (Fig. 3). In addition, the median flushing time as calculated for all stations and sampling times during the winter of 2015–2016 was ~ 5 days (Fig. S14). Previous studies in the NRE noted minimum Chl *a* concentrations during low observed flushing times (2 h to < 10 days), with maximum Chl *a* concentrations measured during a flushing time of ~ 10 days (Peierls et al. 2012; Paerl et al. 2013). We contend that the 10–15% increases in fall and winter precipitation observed over the past 30 years (Easterling et al. 2017) has elevated riverine processes in the NRE, reflected in the increased allochthonous characteristics of DOM and POM following elevated river discharge.

While changes in riverine discharge had a clear impact on the OM pools in the NRE, seasonal changes in temperature were identified as less important drivers, indicating that the dominant climatic drivers in this temperate river-dominated estuary were linked with changes in riverine discharge. Therefore, we expect climate-driven changes in OM cycling in the NRE and other temperate estuaries in the future will likely be a result of changing precipitation patterns as compared to increasing temperature. Indeed, long-term changes in precipitation patterns and amounts, which have been documented for this region (Paerl et al. 2020) have been highlighted as an important control on OM cycling in estuaries in the future by changing the delivery of nutrients leading to changes in primary production in addition to changes in the delivery of allochthonous C (Canuel et al. 2012 and references therein). However, what has yet to be shown is how changes in precipitation as well as evapotranspiration, due to increasing

temperatures in the future, will not only influence riverine discharge but OM cycling as well, especially in temperate estuaries like the NRE (Qi et al. 2009).

Overall, using fluorescence, absorbance, and concentration based metrics to assess both the DOM and POM pools simultaneously in the NRE over an annual timescale revealed that, spatially and temporally, the DOM pool is largely composed of humic-like, terrestrial material delivered from riverine discharge throughout the study period. In contrast, the main source of POM in the NRE was autochthonous planktonic production, as indicated by Chl *a*, with some influence from terrestrial-sources associated with riverine discharge, especially in the upper and mid-estuary. Thus, while DOM is predominantly terrigenous throughout the estuary, the origin of POM in the NRE is spatially explicit, with the upper estuary largely consisting of humic-like, terrestrial material delivered by riverine inflow and the lower estuary being dominated by phytoplankton-mediated primary production. Temporally, results for both OM pools demonstrate the importance of elevated riverine discharge in controlling the quantity and quality of both DOM and POM throughout the estuary, with similar impacts on estuarine OM sources and cycling as following extreme discharge events. This has important implications for our understanding of how OM cycling in estuaries will change in a stormier, high rainfall and riverine discharge future.

**Supplementary Information** The online version contains supplementary material available at <https://doi.org/10.1007/s12237-021-00955-w>.

**Acknowledgements** We thank Betsy Abare, Jeremy Braddy, Lois Kelly, Karen Rossignol, and Randolph Sloup at UNC-CH IMS for assistance with sample collection and analysis. We also thank the co-editor in chief, Dr. Paul Montagna, the associate editor, Dr. Carles Ibanez Martí and two anonymous reviewers for their comments which substantially improved this manuscript.

**Funding** The research was partially supported by a North Carolina USGS-WRRI Fellowship, North Carolina Sea Grant Program (Project R/MG-1505), the North Carolina Department of Environmental Quality/National Fish and Wildlife Foundation (project #8020.16.053916), the Neuse River Estuary Monitoring and Modeling Project (ModMon), and a National Science Foundation Rapid Award (OCE-1705972). In addition, A.G.H.’s time was partially supported by National Science Foundation grants: DEB-1753639, EF-1702506, and CNS-1737424 while at Virginia Tech.

## References

- Arar, E.J., G.B. Collins 1997. In vitro determination of chlorophyll *a* and pheophytin *a* in marine and freshwater algae by fluorescence. EPA Method 445.0. Technical report for USA-EPA, Cincinnati, Ohio, September.
- Asmala, E., H. Kaartokallio, J. Carstensen, and D.N. Thomas. 2016. Variation in riverine inputs affect dissolved organic matter

characteristics throughout the estuarine gradient. *Frontiers in Marine Science* 2 (125). <https://doi.org/10.3389/fmars.2015.00125>.

Asmala, E., L. Haraguchi, S. Markager, P. Massicotte, B. Riemann, P.A. Staehr, and J. Carstensen. 2018. Eutrophication leads to accumulation of recalcitrant autochthonous organic matter in coastal environment. *Global Biogeochemical Cycles* 32 (11): 1673–1687. <https://doi.org/10.1029/2017GB005848>.

Bhattacharya, R., and C.L. Osburn. 2020. Spatial patterns in dissolved organic matter composition controlled by watershed characteristics in a coastal river network: The Neuse River Basin, USA. *Water Research* 169: 115248. <https://doi.org/10.1016/j.watres.2019.115248>.

Borcard, D., F. Gillet, P. Legendre. 2018. *Numerical Ecology with R*, 2nd ed. Springer International Publisher, Cham, Switzerland.

Brym, A., H.W. Paerl, M.T. Montgomery, L.T. Handsel, K. Ziervogel, and C.L. Osburn. 2014. Optical and chemical characterization of base-extracted particulate organic matter in coastal marine environments. *Marine Chemistry* 162: 96–113. <https://doi.org/10.1016/j.marchem.2014.03.006>.

Buzzelli, C.P., R.A. Luettich Jr., S.P. Powers, C.H. Peterson, J.E. McNinch, J.L. Pinckney, and H.W. Paerl. 2002. Estimating the spatial extent of bottom-water hypoxia and habitat degradation in a shallow estuary. *Marine Ecology Progress Series* 230: 103–112.

Canuel, E.A., and A.K. Hardison. 2016. Sources, ages, and alteration of organic matter in estuaries. *Annual Review of Marine Science* 8 (1): 409–434.

Canuel, E.A., S.S. Cammer, H.A. McIntosh, and C.R. Pondell. 2012. Climate change impacts on the organic carbon cycle at the land-ocean interface. *Annual Review of Earth and Planetary Sciences* 40 (1): 685–711. <https://doi.org/10.1146/annurev-earth-042711-105511>.

Christian, R.R., J.N. Boyer, and D.W. Stanley. 1991. Multiyear distribution patterns of nutrients within the Neuse River Estuary, North Carolina. *Marine Ecology Progress Series* 71: 259–274. <https://doi.org/10.3354/meps071259>.

Coble, P.G. 1996. Characterization of marine and terrestrial DOM in seawater using excitation-emission matrix spectroscopy. *Marine Chemistry* 51 (4): 325–346. [https://doi.org/10.1016/0304-4203\(95\)00062-3](https://doi.org/10.1016/0304-4203(95)00062-3).

Dixon, J.L., C.L. Osburn, H.W. Paerl, and B.L. Peierls. 2014. Seasonal changes in estuarine dissolved organic matter due to variable flushing time and wind-driven mixing events. *Estuarine, Coastal and Shelf Science* 151: 210–220. <https://doi.org/10.1016/j.ecss.2014.10.013>.

Dürr, H.H., G.G. Laruelle, C.M. van Kempen, C.P. Slomp, M. Meybeck, and H. Middelkoop. 2011. Worldwide typology of nearshore coastal systems: defining the estuarine filter of river inputs to the oceans. *Estuaries and Coasts* 34 (3): 441–458.

Easterling, D.R., J.R. Arnold, T. Knutson, K.E. Kunkel, A.N. LeGrande, L.R. Leung, R.S. Vose, D.E. Waliser, and M.F. Wehner. 2017. Ch. 7: Precipitation change in the United States. Climate Science Special Report: Fourth National Climate Assessment, Volume I. U.S. Global Change Research Program. <https://doi.org/10.7930/JOH993CC>.

Fellman, J.B., E. Hood, and R.G.M. Spencer. 2010. Fluorescence spectroscopy opens new windows into dissolved organic matter dynamics in freshwater ecosystems: A review. *Limnology and Oceanography* 55 (6): 2452–2462. <https://doi.org/10.4319/lo.2010.55.6.2452>.

Hall, N.S., H.W. Paerl, B.L. Peierls, A.C. Whipple, and K.L. Rossignol. 2013. Effects of climatic variability on phytoplankton community structure and bloom development in the eutrophic, microtidal, New River Estuary, North Carolina, USA. *Estuarine, Coastal and Shelf Science* 117: 70–82. <https://doi.org/10.1016/j.ecss.2012.10.004>.

Hall, N.S., A.C. Whipple, and H.W. Paerl. 2015. Vertical spatio-temporal patterns of phytoplankton due to migration behaviors in two shallow, microtidal estuaries: Influence on phytoplankton function and structure. *Estuarine, Coastal and Shelf Science* 162: 7–21 <https://doi.org/10.1016/j.ecss.2015.03.032>.

Hounshell, A.G., J.C. Rudolph, B.R. Van Dam, N.S. Hall, C.L. Osburn, and H.W. Paerl. 2019. Extreme weather events modulate processing and export of dissolved organic carbon in the Neuse River Estuary, NC. *Estuarine, Coastal, and Shelf Science* 219: 189–200. <https://doi.org/10.1016/j.ecss.2019.01.020>.

Hounshell, A.G., H.W. Paerl, N.S. Hall, J. Braddy, K.L. Rossignol, and R. Sloup. 2021. Time series of environmental parameters and organic matter analyses for dissolved and particulate organic matter in the Neuse River Estuary, North Carolina, USA 2015–2016 Version 1. Environmental Data Initiative. Accessed 2021-03-11. <https://doi.org/10.6073/pasta/76ee76d7ba0e0ef09eb2173cf9d6bd78>.

Huguet, A., L. Vacher, S. Relexans, S. Saubusse, J.M. Froidefond, and E. Parlanti. 2009. Properties of fluorescent dissolved organic matter in the Gironde Estuary. *Organic Geochemistry* 40 (6): 706–719. <https://doi.org/10.1016/j.orggeochem.2009.03.002>.

Jaffé, R., K.M. Cawley, and Y. Yamashita. 2014. Applications of excitation emission matrix fluorescence with parallel factor analysis (EEM-PARAFAC) in assessing environmental dynamics of natural dissolved organic matter (DOM) in aquatic environments: a review, in: Rosario-Ortiz, F. (Ed.), ACS Symposium Series. American Chemical Society, Washington, DC. 27–73. <https://doi.org/10.1021/bk-2014-1160.ch003>.

Janssen, E., R.L. Srivier, D.J. Wuebbles, and K.E. Kunkel. 2016. Seasonal and regional variations in extreme precipitation event frequency using CMIP5. *Geophysical Research Letters* 43 (10): 5385–5393. <https://doi.org/10.1002/2016GL069151>.

Lehmann, J., D. Coumou, and K. Frieler. 2015. Increased record-breaking precipitation events under global warming. *Climatic Change* 132 (4): 501–515.

Letourneau, M.L., and P.M. Medeiros. 2019. Dissolved organic matter composition in a marsh-dominated estuary: Response to seasonal forcing and to the passage of a hurricane. *Journal of Geophysical Research: Biogeosciences* 124 (6): 1545–1559.

Litaker, R.W., P.A. Tester, C.S. Duke, B.E. Kenney, J.L. Pinckney, and J. Ramus. 2002. Seasonal niche strategy of the bloom-forming dinoflagellate *Heterocapsa triquetra*. *Marine Ecology Progress Series* 232: 45–62.

Loh, A.N., J.E. Bauer, and E.A. Canuel. 2006. Dissolved and particulate organic matter source-age characterization in the upper and lower Chesapeake Bay: a combined isotope and biochemical approach. *Limnology and Oceanography* 51 (3): 1421–1431. <https://doi.org/10.4319/lo.2006.51.3.1421>.

Lu, K., and Z. Liu. 2019. Molecular level analysis reveals changes in chemical composition of dissolved organic matter from south Texas rivers after high flow events. *Frontiers in Marine Science* 6: 07. <https://doi.org/10.3389/fmars.2019.000673>.

Luettich, R.A., J.E. McNinch, H.W. Paerl, C.H. Peterson, J.T. Wells, M.J. Alperin, C.S. Martens, and J.L. Pinckney. 2000. Neuse River estuary modeling and monitoring project stage 1: hydrography and circulation, water column nutrients, and productivity, sedimentary processes, and benthic-pelagic coupling, and benthic ecology. Report submitted to NC WRRI. Report no. 325B. Raleigh, NC.

Markager, S., C.A. Stedmon, and M. Søndergaard. 2011. Seasonal dynamics and conservative mixing of dissolved organic matter in the temperate eutrophic estuary Horsens Fjord. *Estuarine, Coastal and Shelf Science* 92 (3): 376–388. <https://doi.org/10.1016/j.ecss.2011.01.014>.

McCallister, S.L., J.E. Bauer, H.W. Ducklow, and E.A. Canuel. 2006. Sources of estuarine dissolved and particulate organic matter: a multi-tracer approach. *Organic Geochemistry* 37 (4): 454–468.

<https://doi.org/10.1016/j.orggeochem.2005.12.005>.

Middelburg, J.J., and P.M.J. Herman. 2007. Organic matter processing in tidal estuaries. *Marine Chemistry* 106 (1-2): 127–147. <https://doi.org/10.1016/j.marchem.2006.02.007>.

Murphy, K.R., C.A. Stedmon, D. Graeber, and R. Bro. 2013. Decomposition routines for Excitation Emission Matrices. *Analytical Methods* 5 (23): 1–29. <https://doi.org/10.1039/c3ay41160e>.

O'Boyle, S., G. McDermott, T. Noklegaard, and R. Wilkes. 2013. A simple index of trophic status in estuaries and coastal bays based on measurements of pH and dissolved oxygen. *Estuaries and Coasts* 36 (1): 158–173. <https://doi.org/10.1007/s12237-012-9553-4>.

Osburn, C.L., L.T. Handsel, M.P. Mikan, H.W. Paerl, and M.T. Montgomery. 2012. Fluorescence tracking of dissolved and particulate organic matter quality in a river-dominated estuary. *Environmental Science & Technology* 46 (16): 8628–8636. <https://doi.org/10.1021/es3007723>.

Osburn, C.L., L.T. Handsel, B.L. Peierls, and H.W. Paerl. 2016. Predicting sources of dissolved organic nitrogen to an estuary from an agro-urban coastal watershed. *Environmental Science & Technology* 50 (16): 8473–8484. <https://doi.org/10.1021/acs.est.6b00053>.

Osburn, C.L., J.C. Rudolph, H.W. Paerl, A.G. Hounshell, and B.R. Van Dam. 2019. Lingering carbon cycle effects of hurricane Matthew in North Carolina's coastal waters. *Geophysical Research Letters* 46 (5): 2654–2661. <https://doi.org/10.1029/2019GL082014>.

Paerl, H.W., J.L. Pinckney, J.M. Fear, and B.L. Peierls. 1998. Ecosystem responses to internal and watershed organic matter loading: consequences for hypoxia in the eutrophying Neuse River Estuary, North Carolina, USA. *Marine Ecological Progress Series* 166: 17–25.

Paerl, H.W., N.S. Hall, B.L. Peierls, K.L. Rossignol, and A.R. Joyner. 2013. Hydrologic variability and its control of phytoplankton community structure and function in two shallow, coastal, lagoonal ecosystems: the Neuse and New River Estuaries, North Carolina, USA. *Estuaries and Coasts* 37 (S1): 31–45. <https://doi.org/10.1007/s12237-013-9686-0>.

Paerl, H.W., J.R. Crosswell, B. Van Dam, N.S. Hall, K.L. Rossignol, C.L. Osburn, A.G. Hounshell, R.S. Sloup, and L.W. Harding. 2018. Two decades of tropical cyclone impacts on North Carolina's estuarine carbon, nutrient and phytoplankton dynamics: implications for biogeochemical cycling and water quality in a stormier world. *Biogeochemistry* 141 (3): 307–332. <https://doi.org/10.1007/s10533-018-0438-x>.

Paerl, H.W., N.S. Hall, A.G. Hounshell, R.A. Luettich, K.L. Rossignol, C.L. Osburn, and J. Bales. 2020. Recent increase in catastrophic tropical cyclone flooding in coastal North Carolina, USA: Long-term observations suggest a regime shift. *Nature Scientific Reports* 9 (1): 10620. <https://doi.org/10.1038/s41598-019-46928-9>.

Peierls, B.L., R.R. Christian, and H.W. Paerl. 2003. Water quality and phytoplankton as indicators of hurricane impacts on a large estuarine ecosystem. *Estuaries* 26 (5): 1329–1343. <https://doi.org/10.1007/BF02803635>.

Peierls, B.L., N.W. Hall, and H.W. Paerl. 2012. Non-monotonic responses of phytoplankton biomass accumulation to hydrologic variability: a comparison of two coastal plain North Carolina estuaries. *Estuaries and Coasts* 35 (6): 1–17. <https://doi.org/10.1007/s12237-012-9547-2>.

Pinckney, J.L., H.W. Paerl, M.B. Harrington, and K.E. Howe. 1998. Annual cycles of phytoplankton community-structure and bloom dynamics in the Neuse River Estuary North Carolina. *Marine Biology* 131 (2): 371–381.

Qi, S., G. Sun, Y. Wang, S.G. McNulty, and J.A. Moore Myers. 2009. Streamflow response to climate and land-use changes in a coastal watershed in North Carolina. *Transactions of the ASABE* 52: 739–749. <https://doi.org/10.13031/2013.27395>.

Raymond, P.A., and J.E. Bauer. 2001. Use of  $^{14}\text{C}$  and  $^{13}\text{C}$  natural abundances for evaluating riverine, estuarine, and coastal DOC and POC sources and cycling: a review and synthesis. *Organic Geochemistry* 32 (4): 469–485. [https://doi.org/10.1016/S0146-6380\(00\)00190-X](https://doi.org/10.1016/S0146-6380(00)00190-X).

Rothenberger, M.B., J.M. Burkholder, and C. Brownie. 2009. Long-term effects of changing land use practices on surface water quality in a coastal river and lagoonal estuary. *Environmental Management* 44 (3): 505–523. <https://doi.org/10.1007/s00267-009-9330-8>.

Rudolph, J.C., C.A. Arendt, A.G. Hounshell, H.W. Paerl, and C.L. Osburn. 2020. Use of geospatial, hydrologic, and geochemical modeling to determine the influence of wetland-derived organic matter in coastal waters in response to extreme weather events. *Frontiers in Marine Science* 7: 18. <https://doi.org/10.3389/fmars.2020.00018>.

Savoye, N., V. David, F. Morisseau, H. Etcheber, G. Abril, I. Billy, K. Charlier, G. Oggian, H. Derriennic, and B. Sautour. 2012. Origin and composition of particulate organic matter in a macrotidal turbid estuary: the Gironde Estuary, France. *Estuarine, Coastal and Shelf Science* 108: 16–28. <https://doi.org/10.1016/j.ecss.2011.12.005>.

Singh, S., P. Dash, M.S. Sankar, S. Silwal, Y. Lu, P. Shang, and R.J. Moorhead. 2019. Hydrological and biogeochemical controls of seasonality in dissolved organic matter delivery to a blackwater estuary. *Estuaries and Coasts* 42 (2): 439–454. <https://doi.org/10.1007/s12237-018-0473-9>.

Spencer, R.G.M., G.R. Aiken, M.M. Dornblaser, K.D. Butler, R.M. Holmes, G. Fiske, P.J. Mann, and A. Stubbins. 2013. Chromophoric dissolved organic matter export from U.S. rivers. *Geophysical Research Letters* 40 (8): 1575–1579. <https://doi.org/10.1002/grl.50357>.

Stedmon, C.A., and S. Markager. 2005. Tracing the production and degradation of autochthonous fractions of dissolved organic matter by fluorescence analysis. *Limnology and Oceanography* 50 (5): 1415–1426. <https://doi.org/10.4319/lo.2005.50.5.1415>.

Thibault, A., S. Derenne, E. Parlanti, C. Anquetil, M. Sourzac, H. Budzinski, L. Fuster, A. Laverma, C. Roose-Amsaleg, E. Viollier, and A. Huguet. 2019. Dynamics of organic matter in the Seine Estuary (France): bulk and structural approaches. *Marine Chemistry* 212: 108–119. <https://doi.org/10.1016/j.marchem.2019.04.007>.

Vlahos, P., and M.M. Whitney. 2017. Organic carbon patterns and budgets in the Long Island Sound estuary. *Limnology and Oceanography* 62 (S1): S46–S57. <https://doi.org/10.1002/lno.10638>.

Weishaar, J.L., M.S. Fram, R. Fujii, and K. Mopper. 2003. Evaluation of specific ultraviolet absorbance as an indicator of the chemical composition and reactivity of dissolved organic carbon. *Environmental Science & Technology* 37 (20): 4702–4708. <https://doi.org/10.1021/es030360x>.